HHS Public Access

Author manuscript

AJR Am J Roentgenol. Author manuscript; available in PMC 2015 December 22.

Published in final edited form as:

AJR Am J Roentgenol. 2015 July ; 205(1): 150–159. doi:10.2214/AJR.14.13632.

Transcranial MR-Guided Focused Ultrasound: A Review of the Technology and Neuro Applications

Pejman Ghanouni, MD, PhD[1], **Kim Butts Pauly, PhD**[2], **W. Jeff Elias, MD**[3], **Jaimie Henderson, MD**[4], **Jason Sheehan, MD**[3], **Stephen Monteith, MD**[5], and **Max Wintermark, MD MAS**[8]

[1]Stanford University, Department of Radiology, Division of Body MRI, Stanford, CA

[2]Stanford University, Departments of Radiology and Electrical Engineering and Bioengineering, Stanford, CA

[3]University of Virginia, Department of Neurosurgery, Charlottesville, VA

[4]Stanford University, Department of Neurosurgery and Neurology and Neurological Sciences, Stanford, CA

[5]Swedish Medical Center, Department of Neurosurgery, Seattle, WA

[7]University of Virginia, Department of Neurosurgery, Charlottesville, VA

[8]Stanford University, Department of Radiology, Division of Neuroradiology, Stanford, CA

Abstract

MR guided focused ultrasound is a new, minimally invasive method of targeted tissue thermal ablation that may be of use to treat central neuropathic pain, essential tremor, Parkinson tremor, and brain tumors. The system has also been used to temporarily disrupt the blood-brain barrier to allow targeted drug delivery to brain tumors. This article reviews the physical principles of MR guided focused ultrasound and discusses current and potential applications of this exciting technology.

Introduction

MR guided focused ultrasound (MRgFUS) is a minimally invasive method of targeted tissue thermal ablation. MRgFUS can also be used for its nonthermal, mechanical effects, e.g. mechanical disruption of blood clots, and for its nonthermal, nonmechanical effects on the excitability of brain cells, i.e. neuromodulation. In all of these approaches, MR imaging is used to localize the target, verify thermal ablation during the procedure, and assess the treatment effects. MRgFUS is used for the treatment of symptomatic uterine fibroids(1) and painful osseous metastases(2), and is under investigation for the treatment of primary cancers in the breast(3) and prostate gland(4). A transcranial MRgFUS system has been developed for treatment of brain lesions through an intact skull(5). This system is used to

Corresponding author and reprint requests: Max Wintermark, MD MAS, Stanford University, Department of Radiology, Division of Neuroradiology, 300 Pasteur Drive, Room S047, Stanford, CA 94305-5105, Phone: (650) 723-7426, Fax: (650) 498-5374, Max.Wintermark@gmail.com.

treat patients with central neuropathic pain(6,7), essential tremor(8), Parkinson tremor(9), and tumors in the brain(10). The system has also been used to temporarily disrupt the bloodbrain barrier to allow targeted drug delivery to the brain in a preclinical study(11). This transcranial MRgFUS system thus has the potential to revolutionize not only functional neurosurgery(12), but also the neurosurgical and pharmacological treatment of brain tumors.

This article will review the physics of transcranial MRgFUS, the typical treatment protocol, and the potential neurological applications, with a focus on imaging findings. Our ultimate goal is to assist the diagnostic radiologist and neurosurgeon to become familiar with the typical imaging patterns after MRgFUS in order to add meaningful value in the multidisciplinary teams caring for patients treated with MRgFUS.

MRgFUS Physical Principles

Equipment

All treatments were done with the transcranial MR guided focused ultrasound (TcMRgFUS) system (ExAblate 4000, InSightec, Tirat Carmel, Israel) shown in Figure 1. At our institution, it integrates with a GE MRI scanner (Milwaukee, WI) operating at 3T, while it can also be coupled to a 1.5T system. The FUS system consists of a 30 cm diameter, hemispheric, 1,024-element phased array transducer operating at 650 kHz. A separate low frequency system operating at 220 kHz is being tested. The device includes a treatment workstation, a front-end electronics unit, an equipment cabinet and a water circulation/ cooling/degassing system. The transducer helmet is housed in a manually operated positioning system and integrated into an MRI table.

Ultrasound focusing

Because of the obstacle it represents to the transmission of ultrasound, the skull creates a number of challenges for targeting the brain with focused ultrasound. Bone attenuates ultrasound energy 20 times more efficiently than soft tissues, with much of that due to absorption, and thus the skull has the potential to heat significantly when exposed to focused ultrasound. The transducer is designed such that there is low intensity over a large area at the transducer surface. Although geometric focusing of the beam results in amplification to achieve a high intensity at a small focal spot, the intensity is still relatively low at the skull as the multiple beams intersect the cranium in different locations, minimizing focal heating on the skull. Despite this distribution of energy, circulating chilled water around the head remains critical to ensure the cranium and adjacent soft tissues do not heat significantly. In addition to attenuation due to the thickness of the bone, there is loss of intensity due to reflections within the trabeculae of the bone and at the interfaces between bone and soft tissue.

The second major issue with the skull is its heterogeneous thickness and density. The speed of sound through bone is higher than that through soft tissues. Since skull thickness is quite variable, the phase of the individual ultrasound beams vary from one another once they pass through different parts of the skull (Figure 2). Because the beams from each transducer element are no longer in phase, they do not sum coherently at the focus. To mitigate this effect, the phase change for each beam path through the skull is estimated and corrected for,

with the result being a more coherent summation of energy at the target(13). Phase correction terms are estimated from a CT scan acquired before the treatment. The CT is registered to the MR acquired at the time of treatment. Phase correction terms are estimated from the path of each ray crossing the skull from the transducer elements to the focus. Phase offsets can also be used to steer the beam within a small range of a few millimeters. For larger changes in focal spot position, the transducer is physically moved, while the patient stays fixed in a frame that is mounted to the MR table and is only in contact with the transducer system though the flexible membrane and water.

Although there is some degree of freedom in the position of the focal spot through moving the transducer and/or electronic focusing, the treatment envelope is at this point still limited to the center of the brain. When the transducer is moved too far in any direction, incidence angles of the beam on the skull are too large. Reflections at these large incidence angles reduce the number of elements that can contribute effectively to the focal spot. The skull base is also a limitation to the treatment envelope. Treatment too near the skull base could result in excessive skull heating(14). Therefore, lesions adjacent to the skull base and to the calvarium cannot currently be treated using MRgFUS.

MR thermal imaging

The intensity at the focal spot may vary between different patients because of a variety of factors: physical factors, such skull thickness and density; technical factors, such as the accuracy of the phase correction; and physiological factors, such as tissue perfusion. As a result, temperature monitoring at the focal spot is critical to verify targeting and adequate heating to achieve ablation.

Many MR parameters change with temperature, including the T1 and T2 decay rates, the proton density, the diffusion coefficient, and the proton resonance frequency. Because it is reversible and linear over the temperature range of interest and easily measured, the change in the proton resonance frequency is the most commonly used parameter for monitoring temperature. The basis for the proton resonance frequency shift is the change in hydrogen bonding seen with temperature. In water, hydrogen bonding pulls the electron cloud away from the protons, so that the protons see a slightly higher magnetic field and precess around the main field a little faster. With a temperature rise, some of those bonds will stretch and break, allowing the electron cloud to shield the protons a little more, reducing the resonance frequency of those protons. On imaging, the average resonance frequency in the voxels is reduced with the temperature rise.

In practice, the change in resonance frequency can be seen in the phase of gradient echo images. Since there are many sources of image phase shifts including field inhomogeneity and susceptibility effects, the temperature-induced change can be isolated by subtracting the phase of a baseline image acquired before the temperature rise. In the simplest implementation, subtracting the phase of the baseline image removes all of the other sources of phase, leaving only the phase that is changing with temperature. An example thermal MR image is shown in Figure 3. MR thermal imaging can be performed in any scan plane, with a sagittal temperature image shown in Figure 3d. As seen in this image, the skull base is located in the far field of the ultrasound beam, but does not heat appreciably(14). When

considering other applications, such as treatment of cortical epilepsy, the heating of the skull base will be a greater concern due to the proximity to the targeted cortical gray matter.

Also evident in the thermal maps of Figure 3 is the small size of the focal spot, which is desirable in applications requiring high precision, such as when targeting specific nuclei in the thalamus. When considering other applications such as brain tumors, the small size of the focal spot will mean numerous sonications will be needed in order to build up a sizable treatment area.

Cavitation detection

Cavitation is the creation and/or collapse of bubbles in tissue. Cavitation is to be avoided because the collapse of bubbles can create large local temperature changes and/or mechanical effects that are undesirable. The likelihood of cavitation increases as the ultrasound frequency decreases. The frequency of 650 kHz was chosen to be low enough to mitigate the severity of the phase aberrations through the skull, while not being so low as to induce cavitation. Nonetheless, cavitation is monitored. Passive cavitation detectors are located inside the transducer (not visible in Figure 2). These are transducer elements that do not transmit ultrasound, but simply listen to ultrasound. The frequency spectrum is displayed adjacent to the temperature monitoring, as shown in Figure 3c. In this plot, all frequency components are below the cavitation threshold dotted line shown.

MR-ARFI

MR-based acoustic radiation force imaging (MR-ARFI) is a new imaging method that will compliment MR-temperature imaging for the precise location of the ablation target(15–17). MR-ARFI may be useful for calibrating the location of the focal spot in the beginning of the procedure. The method relies on the fact that the ultrasound beam imparts a force on the tissue that is proportional to the intensity of the ultrasound beam, and thus greatest at the focus. This force will result in a displacement of the tissue at the focus, shown in Figure 4a. When the ultrasound beam is coincident with a magnetic field gradient, water protons will accumulate a change in phase. Subtraction of images with and without the application of the ultrasound beam reveals the radiation force induced phase in the image in Figure 4d.

Typical patient treatment protocol

Prior to the treatment day, pre-treatment planning images are obtained. These include a CT scan of the entire cranium (0.625 mm slice thickness, helical acquisition, bone kernel, no tilt) and an MRI obtained to define the target. These pre-treatment MR images are registered to the treatment day MRI for delineation of the target.

On the treatment day, the patient’s head is fully shaved, cleaned with alcohol and examined for pre-existing scars or other lesions. An MR compatible stereotactic frame is affixed to the head using screws placed after injection of local anesthesia. The screws are placed as low as possible over the lateral orbits, just above the eyebrows, and in the occipital bone at or below the level of the external occipital protuberance. A circular elastic membrane with a central opening is stretched to fit tightly around the head and placed as low as possible on top of the stereotactic frame. While the patient is being prepared, the TcMRgFUS device is

tested using a gel phantom to ensure proper function. The patient then is positioned supine on the MR table entering the magnet bore. The stereotactic frame is locked to the base plate of the ultrasound transducer on the MR table to maintain a constant relationship between the patient and the transducer. The elastic membrane is fixed to the transducer to achieve a water-tight seal.

The transducer helmet is positioned such that the geometric focus of the transducer is centered on the target zone, using the pre-operative imaging for guidance. Chilled, degassed water is circulated around the patient's head to allow for acoustic coupling of the ultrasound beam to the head and to cool the scalp between sonications. The patient's vital signs are monitored during the treatment. An intravenous line is placed for administration of fluid or medications. Light sedation is sometimes administered. A Foley catheter is recommended due to the length of the procedure. Compression stockings are placed to prevent deep venous thrombosis in the lower limbs. The patient's body temperature is maintained with warming blankets during the procedure. The patient is able to terminate the procedure because of pain or any other reason using a "stop sonication" button.

MR imaging begins with a three-plane localizer, using the body coil. This is followed by a tracking scan that automatically registers the transducer home position using tracking coils embedded in the transducer housing. A scan is then used to determine the central frequency, which is then fixed for to minimize shifts in thermal imaging used for localization of the target. MR imaging, typically including sagittal, axial and coronal T2-weighted fast spin echo imaging, is then performed to confirm the target center. If necessary, the location of the transducer is then readjusted so that the geometric center of the hemispheric transducer is on the target.

The CT images are overlaid on the MR images and used to co-register the current MRI to the previously acquired MR images to assist in precise targeting (Figure 5a and b). Data from the CT scan is also used to provide phase offsets for the transducer elements to compensate for the different density and thickness of the cranium between each transducer element and the intracranial target. The amplitude of the energy from each transducer element is also modified to result in equal acoustic intensity at the skull surface. The treatment planning images are also used to delineate a safe sonication pathway, using CT images to mark intracranial calcifications in the choroid plexus, falx cerebri, basal ganglia or vessels, and using the MR images to demarcate "no pass" regions around the sinuses and any air trapped between the elastic membrane and the scalp (Figure 5c and d), because of the risk of ultrasound absorption and heating in these locations. Fiducial markers are placed on the images along the ventricular and cortical margins to aid in movement detection.

Targeting can be based on an overlaid atlas, or use measurements from an internal reference line. For example, for treatment of essential tremor, one approach for targeting the ventral intermediate nucleus of the thalamus is by measuring 6–7 mm anterior to the posterior commissure and 11 mm laterally from the edge of the third ventricle, at the level of the intercommissural plane connecting the anterior and posterior commissures (Figure 5e). The treatment plan is assessed to confirm that at least 700 elements of the transducer are active,

and that the skull area to be sonicated is at least 250 cm^2, allowing adequate distribution of ultrasound energy over the skull.

Treatment begins with short, low energy sonications performed in the targeted area with sub-therapeutic heating in the 40 – 45°C range. The focus is electronically steered to the point of maximal heating, as assessed in three different planes and frequency directions, correcting any remaining targeting discrepancy. The acoustic power is then slowly increased over several 10–20 second sonications in a verification stage where the size and shape of the sonication spot is evaluated, with temperatures kept between 46 – 50°C. Further treatment to temperatures of 51 – 55°C may generate clinical feedback. This is followed by a higher temperature treatment regime designed to achieve a sufficient thermal dose to achieve thermocoagulation, targeting a 55–60°C peak temperature. Lesion size depends on technical factors such as the time after treatment and the MR imaging method used for measurement, but peak temperatures of 55–60°C typically produce a 4–5 mm diameter region of ablation on T2 weighted MRI obtained the day after treatment. Optimal coverage of the target and clinical feedback from patients both play a role in determining the final peak temperatures. Patients are clinically evaluated after every sonication to assess for symptom suppression and side effects.

Total treatment time spent on the MR table, including positioning, imaging, planning, and sonications is typically three hours. After treatment, the patient is removed from the transducer, and the stereotactic frame is removed. The patient is then returned to the MR table and post-treatment MR images using a head coil are obtained to assess the lesion location and size. A neurological exam is performed after the procedure, and the patient is then monitored in the hospital overnight for any adverse events, with discharge planned for the following morning.

MRgHIFU Applications

Movement disorders and neuropathic pain

Transcranial MRgFUS has been successfully used for the treatment of movement disorders, including essential tremor(8) and Parkinson tremor(9), as well as for the treatment of neuropathic pain(6). All of these are disabling conditions that interfere significantly with patients' quality of life(18) and may be medically refractory. Essential tremor is particularly frequent with an estimated prevalence of 0.3% to 5.55%(19–21). Medically refractory essential tremor can be addressed by lesioning a specific nucleus of the thalamus (ventralis intermedius nucleus (Vim) for tremor(8) and centrolateral thalamus for neuropathic pain(6)). In three recent pilot clinical trials in patients with essential tremor, the Vim nucleus of the thalamus on the contralateral side of their dominant hand was selected as the target for transcranial MRgFUS lesioning(8,22,23). Twenty-seven of 30 patients were successfully treated. With up to 12 months of follow-up in the largest trial, the studies reported significant improvements in tremor, disability and quality of life. Complications related to MRgFUS thalamotomy included paresthesias of the face or fingers, which persisted at 12 months in 5 of 19 patients, persistent dysesthesia of the index finger in one patient, and transient unsteadiness, ataxia, dysmetria, grip weakness, and slurred speech, all of which resolved within a month. Stereotactic radiofrequency thalamotomy and deep brain

stimulation (DBS) are also effective methods for treating essential tremor, with RF thalamotomy resulting in tremor relief in 73–93% and DBS successfully eliminating tremor in 42–90%(24,25). Tolerance to thalamic DBS has been reported in up to 30% of patients. Both RF thalamotomy and DBS require a craniotomy. These procedures may be complicated by paresthesias in 20% at 12 months, intracranial hemorrhage (1–3%), neurological deficits in 1–2%, and infection in 5–10%(26,27). Stereotactic radiosurgery is also used for treatment of tremor, with studies reporting clinical improvement in 70–90%(28,29). Radiosurgery is limited by delayed onset of effect and does not allow for immediate verification of targeting, which may limit effectiveness or result in complications depending on the accuracy of targeting. Reported side effects include paresthesia, hemiparesis, speech impairment, and hemorrhage, with complication rates reported between 1.3–8.7%(30).

Typical imaging findings can be observed at the transcranial MRgFUS target site(31)(Figure 6). At 24 hours, a lesion can be seen with restricted diffusion and low ADC values at its center (Zone 2). On T2-weighted imaging, Zone 1 is hypointense, surrounded by a strongly hyperintense Zone 2 demarcated by a hypointense rim. Zones 1 and 2 represent coagulation necrosis and cytotoxic edema(32–34). Finally, the poorly marginated, slightly hyperintense Zone 3 at the periphery represents vasogenic edema(34,35). Zone 3 is typically seen between 24 hours and 1 week, and then resolves. Zones 1 and 2 evolve into a round or oval cavity at 1 week and 1 month, and collapse by 3 months. Small amounts of blood products but no frank hemorrhage are seen at the target site immediately after the MRgFUS treatment and afterwards. A few patients displayed very mild and transient enhancement at the target site at 24 hours, likely resulting from the reversible alteration of the blood-brain barrier caused by the MRgFUS treatment(36). Enhancement reappeared by 1 week and peaked at 1 month, possibly related to neovascularization(37).

The imaging pattern and histology of MRgFUS lesions resembles what is seen for other thermal lesioning modalities like stereotactic radiofrequency thalamotomies, but are quite different from those observed with gammaknife radiosurgery(33,38). MRgFUS has many potential advantages over stereotactic radiofrequency thalamotomies and stereotactic radiosurgery as a transcranial, non-radiation lesioning method. MRgFUS is characterized by a sharp thermal gradient, creating a more focal effect as compared to the broader gradient of radiation dose. Theoretically, MRgFUS produces a sharply delineated lesion from homogeneous thermal dose, while radiofrequency heating dissipates with distance from a central lesioning electrode. One imaging manifestation of this observation is that there is usually more vasogenic edema around radiofrequency lesions compared to MRgFUS lesions(33). Compared to MRgFUS and radiofrequency ablation, stereotactic radiosurgery has the disadvantage of latent treatment effects and the possibility of more extensive tissue damage beyond the intended target(33).

On diffusion tensor imaging, continuous decreased fractional anisotropy (FA) can be seen over time at the site of thalamotomy, but also distant from it, in the following regions or structures: ipsilateral precentral and postcentral subcortical white matter in the hand knob area, corticospinal tract in the ipsilateral centrum semi-ovale, posterior arm of the ipsilateral internal capsule and ipsilateral cerebral peduncle, contralateral middle cerebellar peduncle,

and bilateral superior vermis (39). It is hypothesized that this decrease of FA values over time represents a degeneration of neuronal circuits, triggered by the thalamic lesion induced by the MRgFUS treatment. Two circuits involving the structures listed above and thought to contribute to the essential tremor pathophysiology are the Guillain-Mollaret triangle(40–45) and the dento-rubro-thalamo-cortical tract(46,47).

The clinical response of the tremor to the MRgFUS was influenced by the size of the lesion, including the surrounding vasogenic edema(31). Tremor improvement slightly receded after the vasogenic edema surrounding the lesion resolved, but there was nevertheless persistent clinical improvement 1 year after the MRgFUS treatment. In most cases, the lesion collapsed at 3 months(31), while in other cases, the lesion persisted to one year(7). Also, we observed a correlation between the slope of FA decrease over time and the degree of clinical improvement of essential tremor(39).

Trigeminal neuralgia is a clinical condition consisting of a temporary paroxysmal pain in the trigeminal nerve distribution typically confined to one side of the face(48). Patients with trigeminal neuralgia are treated with drugs including gabapentin, carbamazepine, baclofen and pregabalin. If medical treatment fails, patients are referred for neurosurgical microvascular decompression(49), as the pain is thought to be caused by vascular impingement on the trigeminal nerve. Percutaneous injection and radiofrequency ablation have also been used as treatment modalities, as well as stereotactic radiosurgery(48). Stereotactic radiosurgery typically targets the root entry zone, and it has been demonstrated in human cadavers that MRgFUS can also be used for this purpose(50). This application remains to be validated in patients. Imaging findings after MRgFUS lesioning of the root entry zone of the trigeminal nerve show increased T2-signal and transient enhancement(50).

Intracranial hemorrhage and ischemic stroke

Each year in the United States, 40,000 patients suffer an intracranial hemorrhage, and a third of them die within the first 30 days, usually because of mass effect and herniation caused by the intracranial hematoma(51–53). The treatment of intracranial hemorrhage is medical, with surgical evacuation of the hematoma reserved for cerebellar hemorrhage that causes rapid neurologic deterioration, brainstem compression, or hydrocephalus, and sometimes also for large supratentorial hematoma(54). Because of the concern that surgical evacuation may damage the surrounding normal brain parenchyma, minimally invasive clot evacuation techniques utilizing endoscopic or stereotactic aspiration have been proposed, with a typical therapeutic window spanning up to 48 hours after onset(55–57). The Minimally-Invasive Surgery plus rtPA for Intracerebral Hemorrhage Evacuation (MISTIE) trial demonstrated that stereotactic catheter aspiration followed by tPA administration resulted in a 50% reduction in clot volume without significantly increasing the incidence of adverse events versus 6% in the medical arm(58). The Clot Lysis Evaluating Accelerated Resolution of Intraventricular Hemorrhage (CLEAR-IVH) clinical trial showed that intraventricular tPA administration accelerates clot lysis, improving cereobrospinal fluid drainage and reduces hydrocephalus(59). MRgFUS is considered as a potential noninvasive treatment modality for intracranial hemorrhage, due to its ability to break down clot by inertial cavitation and mechanical forces(60).

The imaging appearance of intracranial hematomas and its dependence on time is well known. However, this classical description is suboptimal for MRgFUS sonothrombolysis, because of the considered time window, which is a matter of hours (as mentioned above), not days, weeks or months, and because of the need to differentiate between solid and liquid phases rather than oxygenation state of hemoglobin(61–63).

In a phantom study using human blood, the pre-sonication clot was hyperintense on T1- and hypointense on T2- and T2*-weighted MR images, due to the conversion of hemoglobin to deoxyhemoglobin with retraction of the clot. After sonication, the T1 signal was grossly unchanged while the T2 and T2* signal was increased. On T2-weighted images, the postsonication samples looked like serum, corresponding to the near complete hemolytic release of hemoglobin degradation products in the extracellular fluid, as seen on histology(64). T2-weighted imaging is the optimum imaging sequence for intraoperative monitoring of MRgFUS sonothrombolysis of intracranial hemorrhage. T2* may represent an alternative but is more difficult to use intraoperatively because of susceptibility artifacts.

Clinical use of ultrasound to augment the use of tPA has been widely used in the treatment of acute ischemic stroke. In a meta-analysis of 9 trials (416 patients), Tsivgoulis et al. showed higher recanalization rates in patients receiving transcranial doppler and tPA (37.2%) compared with tPA alone (17.2%)(65). It is conceivable that MRgFUS might help increase these recanalization rates even higher, because it can be focused on clots in proximal arteries and facilitate the quick dissolution of such clots (Figure 7). There are obviously major logistic hurdles that will need to be overcome so that MRgFUS treatment of ischemic stroke can be implemented in a timely fashion without delaying stroke treatment, respecting the fundamental principle that “time is brain”.

Treatment of brain tumors

Thermal ablation of gliomas was performed in three patients who had local recurrence after standard surgical resection and radiation therapy(32). These FUS procedures were carried out through a craniotomy to create an acoustic window, with 50% of the enhancing tumor volume ablated in one patient, and resolution of nearly all tumoral enhancement in a second. Complications included off-target ablation in the midbrain resulting in hemiparesis. Another three patients with inoperable gliomas were treated with FUS through an intact cranium(10). Because of power limitations of this version of the device, ablative temperatures were not achieved. A modified version of this device, operating at a lower frequency, was used in a fourth patient, but treatment was complicated by intracranial hemorrhage and death. Cavitation was thought to be a likely cause for the intracranial hemorrhage. Recently, a patient with a metastatic brain tumor and another patient with recurrent glioblastoma successfully received limited treatment with the mid-frequency tcMRgFUS device(66,67).

In addition to thermal therapy, focused ultrasound can also be used to non-invasively and transiently disrupt the blood brain barrier(68). Most systemically administered drugs cannot cross the blood-brain barrier (BBB), which both limits transport of molecules based on their size, polarity and hydrophilicity, and also actively removes chemotherapeutic agents from the brain(69–72). Methods have been explored to enhance delivery of therapeutic agents to tumors in the brain, including chemical modification of the agents so that they cross the

BBB(70), intratumoral injection, convection-enhanced delivery, and combined intra-arterial delivery of drugs with osmotic agents that can globally disrupt the BBB(71,73,74).

BBB permeability is consistently enhanced through mechanical effects of focused ultrasound on injected microbubbles(75,76). When exposed to ultrasound waves, the intravascular microbubbles generate mechanical forces on the vessel walls that focally open the BBB(72,74,77,78). The ultrasound intensity needed to disrupt the BBB in the presence of microbubbles is much less than what is needed for thermal ablation, so there is no significant heating of the skull with this approach, and no significant injury to the brain parenchyma or vasculature(11,77,79,80).

Studies using experimental animal tumor models have demonstrated the ability of focused ultrasound to increase the concentration of therapeutic agents in the brain. After focused ultrasound mediated disruption of the BBB in rat brain, doxorubicin crossed into the brain parenchyma(81) and delayed the growth of implanted gliomas(73). The antibody trastuzumab was delivered to the brain after BBB disruption in rats(76), and resulted in decreased volume of implanted HER2/neu positive breast cancer metastases and improved survival. Similar FUS-mediated methods of BBB opening have increased delivery of BCNU(82) and temozolomide(83) to rat brains implanted with glioblastomas, resulting in decreased tumor size and prolonged survival.

These methods have been extended to primates, with FUS used to safely, reproducibly, and focally disrupt the BBB in rhesus macaques, potentially allowing for non-invasive and repeated delivery of drugs to the human brain(11). This may be particularly useful in the treatment of malignant gliomas, which, because of its infiltration into the brain parenchyma, has not responded well to conventional treatment methods(5,12,84).

For tumor applications, the high frequency MRgFUS system has too small of a treatment envelope as tumors are not confined to the central region of the brain. Successful application of MRgFUS will require expansion of the treatment envelope through the use of low frequency MRgFUS. Ongoing work to improve cavitation detection and avoidance with the low frequency system is underway.

Limitations

MR guided focused ultrasound is approved in the United States as a technique for the treatment of uterine fibroids and of painful osseous metastases. Although the transcranial MRgFUS system has been Conformité Européene-approved for the treatment of essential tremor, Parkinson disease and neuropathic pain, it has been applied clinically to the fields of stereotactic and functional neurosurgery in a limited number of institutions. Although ongoing clinical trials in the United States are investigating transcranial MRgFUS for the treatment of Parkinson disease, for the ablation of brain metastases, and for the delivery of chemotherapy to glioblastomas by opening the blood-brain barrier, the feasibility of tcMRgFUS for these applications has not been confirmed.

Conclusion

MR guided focused ultrasound is a nascent technology with current and potential intracranial applications including functional neurosurgery, relief of neuropathic pain, tumor ablation, drug delivery, and thrombolysis. There is an ongoing randomized, placebo controlled Phase 3 study using MRgFUS to treat essential tremor, and similar testing is needed to validate these and other neuro applications of MRgFUS. In addition, improved imaging techniques must be developed to aid in targeting and evaluation of clinical outcomes.

Bibliography

1. Trumm CG, Stahl R, Clevert D-A, Herzog P, Mindjuk I, Kornprobst S, et al. Magnetic resonance imaging-guided focused ultrasound treatment of symptomatic uterine fibroids: impact of technology advancement on ablation volumes in 115 patients. Invest Radiol. 2013 Jun; 48(6):359–365. [PubMed: 23385396]
2. Hurwitz MD, Ghanouni P, Kanaev SV, Iozeffi D, Gianfelice D, Fennessy FM, et al. Magnetic Resonance-Guided Focused Ultrasound for Patients With Painful Bone Metastases: Phase III Trial Results. JNCI Journal of the National Cancer Institute. 2014 May 14.106(5) dju082-2.
3. Schmitz AC, Gianfelice D, Daniel BL, Mali WPTM, Bosch MAAJ. Image-guided focused ultrasound ablation of breast cancer: current status, challenges, and future directions. Eur Radiol. 2008 Mar 20; 18(7):1431–1441. [PubMed: 18351348]
4. Napoli A, Anzidei M, De Nunzio C, Cartocci G, Panebianco V, De Dominicis C, et al. Real-time Magnetic Resonance–guided High-intensity Focused Ultrasound Focal Therapy for Localised Prostate Cancer: Preliminary Experience. European Urology. 2013 Feb; 63(2):395–398. [PubMed: 23159454]
5. Jolesz FA, McDannold NJ. Magnetic Resonance–Guided Focused Ultrasound. Neurologic Clinics of NA. Elsevier Inc. 2014 Feb 1; 32(1):253–269.
6. Martin E, Jeanmonod D, Morel A, Zadicario E, Werner B. High-intensity focused ultrasound for noninvasive functional neurosurgery. Ann Neurol. 2009 Dec; 66(6):858–861. [PubMed: 20033983]
7. Jeanmonod D, Werner B, Morel A, Michels L, Zadicario E, Schiff G, et al. Transcranial magnetic resonance imaging–guided focused ultrasound: noninvasive central lateral thalamotomy for chronic neuropathic pain. Neurosurg Focus. 2012 Jan.32(1):E1. [PubMed: 22208894]
8. Elias WJ, Huss D, Voss T, Loomba J, Khaled M, Zadicario E, et al. A Pilot Study of Focused Ultrasound Thalamotomy for Essential Tremor. N Engl J Med. 2013 Aug 15; 369(7):640–648. [PubMed: 23944301]
9. Magara A, hler RB, Moser D, Kowalski M, Pourtehrani P, Jeanmonod D. First experience with MR-guided focused ultrasound in the treatment of Parkinson's disease. 2014 May 31; 2(1):1–8.
10. McDannold N, Clement GT, Black P, Jolesz F, Hynynen K. Transcranial Magnetic Resonance Imaging– Guided Focused Ultrasound Surgery of Brain Tumors. Neurosurgery. 2010 Feb; 66(2): 323–332. [PubMed: 20087132]
11. McDannold N, Arvanitis CD, Vykhodtseva N, Livingstone MS. Temporary Disruption of the Blood-Brain Barrier by Use of Ultrasound and Microbubbles: Safety and Efficacy Evaluation in Rhesus Macaques. Cancer Res. 2012 Jul 15; 72(14):3652–3663. [PubMed: 22552291]
12. Monteith S, Sheehan J, Medel R, Wintermark M, Eames M, Snell J, et al. Potential intracranial applications of magnetic resonance–guided focused ultrasound surgery. Journal of Neurosurgery. 2013 Feb; 118(2):215–221. [PubMed: 23176339]
13. Clement GT, White PJ, King RL, McDannold N, Hynynen K. A magnetic resonance imaging-compatible, large-scale array for trans-skull ultrasound surgery and therapy. J Ultrasound Med. 2005 Aug; 24(8):1117–1125. [PubMed: 16040827]
14. Pulkkinen A, Huang Y, Song J, Hynynen K. Simulations and measurements of transcranial low-frequency ultrasound therapy: skull-base heating and effective area of treatment. Phys Med Biol. 2011 Jul 6; 56(15):4661–4683. [PubMed: 21734333]

15. McDannold N, Maier SE. Magnetic resonance acoustic radiation force imaging. Med Phys. 2008; 35(8):3748. [PubMed: 18777934]
16. Kaye EA, Pauly KB. Adapting MRI acoustic radiation force imaging for in vivo human brain focused ultrasound applications. Magn Reson Med. 2013 Mar; 69(3):724–733. [PubMed: 22555751]
17. Radicke M, Engelbertz A, Habenstein B, Lewerenz M, Oehms O, Trautner P, et al. New image contrast method in magnetic resonance imaging via ultrasound. Hyperfine Interact. 2008 Aug 1; 181(1–3):21–26.
18. Lorenz D, Schwieger D, Moises H, Deuschl G. Quality of life and personality in essential tremor patients. Mov Disord. 2006; 21(8):1114–1118. [PubMed: 16622851]
19. Bharucha NE, Bharucha EP, Bharucha AE, Bhise AV, Schoenberg BS. Prevalence of essential tremor in the Parsi community of Bombay, India. Arch Neurol. 1988 Aug; 45(8):907–908. [PubMed: 3270998]
20. Haerer AF, Anderson DW, Schoenberg BS. Prevalence of essential tremor. Results from the Copiah County study. Arch Neurol. 1982 Dec; 39(12):750–751. [PubMed: 7138316]
21. Rajput AH, Offord KP, Beard CM, Kurland LT. Essential tremor in Rochester, Minnesota: a 45-year study. J Neurol Neurosurg Psychiatr. 1984 May; 47(5):466–470. [PubMed: 6736976]
22. Lipsman N, Schwartz ML, Huang Y, Lee L, Sankar T, Chapman M, et al. MR-guided focused ultrasound thalamotomy for essential tremor: a proof-of-concept study. The Lancet Neurology. Elsevier Ltd. 2013 Apr 12; 12(5):462–468.
23. Chang WS, Jung HH, Kweon EJ, Zadicario E, Rachmilevitch I, Chang JW. Unilateral magnetic resonance guided focused ultrasound thalamotomy for essential tremor: practices and clinicoradiological outcomes. J Neurol Neurosurg Psychiatr. 2014 May 29.
24. Pahwa R, Lyons KE, Wilkinson SB, Tröster AI, Overman J, Kieltyka J, et al. Comparison of thalamotomy to deep brain stimulation of the thalamus in essential tremor. Mov Disord. 2001 Jan; 16(1):140–143. [PubMed: 11215575]
25. Schuurman PR, Bosch DA, Bossuyt PM, Bonsel GJ, van Someren EJ, de Bie RM, et al. A comparison of continuous thalamic stimulation and thalamotomy for suppression of severe tremor. N Engl J Med. 2000 Feb 17; 342(7):461–468. [PubMed: 10675426]
26. Tasker RR. Deep brain stimulation is preferable to thalamotomy for tremor suppression. Surg Neurol. 1998 Feb; 49(2):145–53. discussion 153–4. [PubMed: 9457264]
27. Chan DTM, Zhu XL, Yeung JHM, Mok VCT, Wong E, Lau C, et al. Complications of Deep Brain Stimulation: A Collective Review. Asian Journal of Surgery. Asian Surgical Association. 2009 Oct 1; 32(4):258–263.
28. Kondziolka D, Ong JG, Lee JYK, Moore RY, Flickinger JC, Lunsford LD. Gamma Knife thalamotomy for essential tremor. Journal of Neurosurgery. 2008 Jan; 108(1):111–117. [PubMed: 18173319]
29. Kooshkabadi A, Lunsford LD, Tonetti D, Flickinger JC, Kondziolka D. Gamma Knife thalamotomy for tremor in the magnetic resonance imaging era. Journal of Neurosurgery. 2013 Apr; 118(4):713–718. [PubMed: 23373801]
30. Young RF, Li F, Vermeulen S, Meier R. Gamma Knife thalamotomy for treatment of essential tremor: long-term results. Journal of Neurosurgery. 2010 Jun; 112(6):1311–1317. [PubMed: 19895197]
31. Wintermark M, Druzgal J, Huss DS, Khaled MA, Monteith S, Raghavan P, et al. Imaging Findings in MR Imaging-Guided Focused Ultrasound Treatment for Patients with Essential Tremor. American Journal of Neuroradiology. 2013 Dec 26; 35(5):891–896. [PubMed: 24371027]
32. Ram Z, Cohen ZR, Harnof S, Tal S, Faibel M, Nass D, et al. Magnetic resonance imaging-guided, high-intensity focused ultrasound for brain tumor therapy. Neurosurgery. 2006 Nov; 59(5):949–55. discussion 955–6. [PubMed: 17143231]
33. Elias WJ, Khaled M, Hilliard JD, Aubry J-F, Frysinger RC, Sheehan JP, et al. A magnetic resonance imaging, histological, and dose modeling comparison of focused ultrasound, radiofrequency, and Gamma Knife radiosurgery lesions in swine thalamus. Journal of Neurosurgery. 2013 Aug; 119(2):307–317. [PubMed: 23746105]

34. Chen L, Bouley DM, Harris BT, Butts K. MRI study of immediate cell viability in focused ultrasound lesions in the rabbit brain. J Magn Reson Imaging. 2001 Jan; 13(1):23–30. [PubMed: 11169799]
35. Hynynen K, McDannold N, Clement G, Jolesz FA, Zadicario E, Killiany R, et al. Pre-clinical testing of a phased array ultrasound system for MRI-guided noninvasive surgery of the brain—A primate study. European Journal of Radiology. 2006 Aug; 59(2):149–156. [PubMed: 16716552]
36. Hynynen K, McDannold N, Vykhodtseva N, Jolesz FA. Non-invasive opening of BBB by focused ultrasound. Acta Neurochir Suppl. 2003; 86:555–558. [PubMed: 14753505]
37. Smirniotopoulos JG, Murphy FM, Rushing EJ, Rees JH, Schroeder JW. From the Archives of the AFIP: Patterns of Contrast Enhancement in the Brain and Meninges. Radiographics. 2007 Mar 1; 27(2):525–551. [PubMed: 17374867]
38. Tomlinson FH, Jack CR, Kelly PJ. Sequential magnetic resonance imaging following stereotactic radiofrequency ventralis lateralis thalamotomy. Journal of Neurosurgery. 1991 Apr; 74(4):579–584. [PubMed: 2002371]
39. Wintermark M, Huss DS, Shah BB, Tustison N, Druzgal TJ, Kassell N, et al. Thalamic Connectivity in Patients with Essential Tremor Treated with MR Imaging-guided Focused Ultrasound: In Vivo Fiber Tracking by Using Diffusion-Tensor MR Imaging. Radiology. 2014 Mar.
40. Dupuis MJ, Delwaide PJ, Boucquey D, Gonsette RE. Homolateral disappearance of essential tremor after cerebellar stroke. Mov Disord. 1989; 4(2):183–187. [PubMed: 2733709]
41. Jia L, Jia-lin S, Qin D, Qing L, Yan Z. A Diffusion Tensor Imaging Study in Essential Tremor. Journal of Neuroimaging. 2010 Nov 17; 21(4):370–374. [PubMed: 21091815]
42. Colebatch JG, Findley LJ, Frackowiak RS, Marsden CD, Brooks DJ. Preliminary report: activation of the cerebellum in essential tremor. The Lancet. 1990 Oct 27; 336(8722):1028–1030.
43. Wills AJ, Jenkins IH, Thompson PD, Findley LJ, Brooks DJ. A positron emission tomography study of cerebral activation associated with essential and writing tremor. Arch Neurol. 1995 Mar; 52(3):299–305. [PubMed: 7872885]
44. Wills AJ, Jenkins IH, Thompson PD, Findley LJ, Brooks DJ. Red nuclear and cerebellar but no olivary activation associated with essential tremor: a positron emission tomographic study. Ann Neurol. 1994 Oct; 36(4):636–642. [PubMed: 7944296]
45. Urushitani M, Inoue H, Kawamura K, Kageyama T, Fujisawa M, Nishinaka K, et al. Disappearance of essential neck tremor after pontine base infarction. No To Shinkei. 1996 Aug; 48(8):753–756. [PubMed: 8797210]
46. Nicoletti G, Manners D, Novellino F, Condino F, Malucelli E, Barbiroli B, et al. Diffusion tensor MRI changes in cerebellar structures of patients with familial essential tremor. Neurology. 2010 Mar 22; 74(12):988–994. [PubMed: 20308683]
47. Shin DH, Han BS, Kim HS, Lee PH. Diffusion Tensor Imaging in Patients With Essential Tremor. American Journal of Neuroradiology. 2008 Jan 1; 29(1):151–153. [PubMed: 17921227]
48. Bennetto L, Patel NK, Fuller G. Trigeminal neuralgia and its management. BMJ. 2007 Jan 27; 334(7586):201–205. [PubMed: 17255614]
49. TAARNHØJ P. Decompression of the trigeminal root and the posterior part of the ganglion as treatment in trigeminal neuralgia; preliminary communication. Journal of Neurosurgery. 1952 May; 9(3):288–290. [PubMed: 14939059]
50. Monteith SJ, Medel R, Kassell NF, Wintermark M, Eames M, Snell J, et al. Transcranial magnetic resonance–guided focused ultrasound surgery for trigeminal neuralgia: a cadaveric and laboratory feasibility study. Journal of Neurosurgery. 2013 Feb; 118(2):319–328. [PubMed: 23157185]
51. Sacco S, Marini C, Toni D, Olivieri L, Carolei A. Incidence and 10-Year Survival of Intracerebral Hemorrhage in a Population-Based Registry. Stroke. 2009 Jan 26; 40(2):394–399. [PubMed: 19038914]
52. Gebel JM, Broderick JP. Intracerebral hemorrhage. Neurologic Clinics of NA. 2000 May; 18(2): 419–438.
53. Lovelock CE, Molyneux AJ, Rothwell PM. Change in incidence and aetiology of intracerebral haemorrhage in Oxfordshire, UK, between 1981 and 2006: a population-based study. The Lancet Neurology. 2007 Jun; 6(6):487–493. [PubMed: 17509483]

54. Morgenstern LB, Hemphill JC, Anderson C, Becker K, Broderick JP, Connolly ES, et al. Guidelines for the Management of Spontaneous Intracerebral Hemorrhage: A Guideline for Healthcare Professionals From the American Heart Association/American Stroke Association. Stroke. 2010 Aug 30; 41(9):2108–2129. [PubMed: 20651276]
55. Teernstra OPM, Evers SMAA, Lodder J, Leffers P, Franke CL, Blaauw G. Stereotactic Treatment of Intracerebral Hematoma by Means of a Plasminogen Activator: A Multicenter Randomized Controlled Trial (SICHPA). Stroke. 2003 Apr 1; 34(4):968–974. [PubMed: 12649510]
56. Wang W-Z, Jiang B, Liu H-M, Li D, Lu C-Z, Zhao Y-D, et al. Minimally invasive craniopuncture therapy vs. conservative treatment for spontaneous intracerebral hemorrhage: results from a randomized clinical trial in China. Int J Stroke. 2009 Feb; 4(1):11–16. [PubMed: 19236490]
57. Auer LM, Deinsberger W, Niederkorn K, Gell G, Kleinert R, Schneider G, et al. Endoscopic surgery versus medical treatment for spontaneous intracerebral hematoma: a randomized study. Journal of Neurosurgery. 1989 Apr; 70(4):530–535. [PubMed: 2926492]
58. Morgan T, Zuccarello M, Narayan R, Keyl P, Lane K, Hanley D. Preliminary findings of the minimally-invasive surgery plus rtPA for intracerebral hemorrhage evacuation (MISTIE) clinical trial. Acta Neurochir Suppl. 2008; 105:147–151. [PubMed: 19066101]
59. Morgan T, Awad I, Keyl P, Lane K, Hanley D. Preliminary report of the clot lysis evaluating accelerated resolution of intraventricular hemorrhage (CLEARIVH) clinical trial. Acta Neurochir Suppl. 2008; 105:217–220. [PubMed: 19066112]
60. Harnof S, Zibly Z, Hananel A, Monteith S, Grinfeld J, Schiff G, et al. Potential of Magnetic Resonance-guided Focused Ultrasound for Intracranial Hemorrhage: An In Vivo Feasibility Study. Journal of Stroke and Cerebrovascular Diseases. Elsevier Ltd. 2014 Apr.4:1–7.
61. Bryant RG, Marill K, Blackmore C, Francis C. Magnetic relaxation in blood and blood clots. Magn Reson Med. 1990 Jan; 13(1):133–144. [PubMed: 2319929]
62. Gomori JM, Grossman RI. Mechanisms responsible for the MR appearance and evolution of intracranial hemorrhage. Radiographics. 1988 May; 8(3):427–440. [PubMed: 3380989]
63. Bradley WG. MR appearance of hemorrhage in the brain. Radiology. 1993 Oct; 189(1):15–26. [PubMed: 8372185]
64. Durst C, Monteith S, Sheehan J, Moldovan K, Snell J, Eames M, et al. Optimal imaging of in vitro clot sonothrombolysis by MR-guided focused ultrasound. J Neuroimaging. 2013 Apr; 23(2):187–191. [PubMed: 22082153]
65. Tsivgoulis G, Eggers J, Ribo M, Perren F, Saqqur M, Rubiera M, et al. Safety and efficacy of ultrasound-enhanced thrombolysis: a comprehensive review and meta-analysis of randomized and nonrandomized studies. Stroke. 2010 Feb; 41(2):280–287. [PubMed: 20044531]
66. Fandino, J.; Coluccia, D.; Schwyzer, L.; Anon, J.; Remonda, L.; O'Gormann, R., et al. First Non-Invasive Thermal Ablation of a Brain Tumor with MR guided Focused Ultrasound. Current and Future Application of Focused Ultrasound; Bethesda MD. 4th International Symposium; 2014.
67. Monteith, S.; Newell, D.; Vermeulen, S.; Cobbs, C. Clinical Trial Update: Treatment of Metastatic Brain Tumors Using MRgFUS. Current and Future Application of Focused Ultrasound; 4th International Symposium; Bethesda, MD. 2014.
68. Park E-J, Zhang Y-Z, Vykhodtseva N, McDannold N. Ultrasound-mediated blood-brain/blood-tumor barrier disruption improves outcomes with trastuzumab in a breast cancer brain metastasis model. Journal of Controlled Release. 2012 Nov; 163(3):277–284. [PubMed: 23000189]
69. Abbott NJ, Romero IA. Transporting therapeutics across the blood-brain barrier. Mol Med Today. 1996 Mar; 2(3):106–113. [PubMed: 8796867]
70. Pardridge WM. Drug and gene delivery to the brain: the vascular route. Neuron. 2002 Nov 14; 36(4):555–558. [PubMed: 12441045]
71. Misra A, Ganesh S, Shahiwala A, Shah SP. Drug delivery to the central nervous system: a review. J Pharm Pharm Sci. 2003 May; 6(2):252–273. [PubMed: 12935438]
72. Etame AB, Diaz RJ, Smith CA, Mainprize TG, Hynynen K, Rutka JT. Focused ultrasound disruption of the blood-brain barrier: a new frontier for therapeutic delivery in molecular neurooncology. Neurosurg Focus. 2012 Jan.32(1):E3. [PubMed: 22208896]

73. Liu H-L, Yang H-W, Hua M-Y, Wei K-C. Enhanced therapeutic agent delivery through magnetic resonance imaging–monitored focused ultrasound bloodbrain barrier disruption for brain tumor treatment: an overview of the current preclinical status. Neurosurg Focus. 2012 Jan.32(1):E4.
74. Colen RR, Jolesz FA. Future Potential of MRI-Guided Focused Ultrasound Brain Surgery. Neuroimaging Clinics of NA Elsevier Ltd. 2010 Aug 1; 20(3):355–366.
75. Hynynen K, McDannold N, Vykhodtseva N, Jolesz FA. Noninvasive MR Imaging–guided Focal Opening of the Blood-Brain Barrier in Rabbits1. Radiology. 2001 Sep; 220(3):640–646. [PubMed: 11526261]
76. Kinoshita M, McDannold N, Jolesz FA, Hynynen K. Noninvasive localized delivery of Herceptin to the mouse brain by MRI-guided focused ultrasoundinduced blood-brain barrier disruption. Proc Natl Acad Sci USA. 2006 Aug 1; 103(31):11719–11723. [PubMed: 16868082]
77. Hynynen K, McDannold N, Vykhodtseva N, Raymond S, Weissleder R, Jolesz FA, et al. Focal disruption of the blood-brain barrier due to 260-kHz ultrasound bursts: a method for molecular imaging and targeted drug delivery. Journal of Neurosurgery. 2006 Sep; 105(3):445–454. [PubMed: 16961141]
78. Sheikov N, McDannold N, Vykhodtseva N, Jolesz F, Hynynen K. Cellular mechanisms of the blood-brain barrier opening induced by ultrasound in presence of microbubbles. Ultrasound in Medicine & Biology. 2004 Jul; 30(7):979–989. [PubMed: 15313330]
79. Hynynen K, Pomeroy O, Smith DN, Huber PE, McDannold NJ, Kettenbach J, et al. MR imaging-guided focused ultrasound surgery of fibroadenomas in the breast: a feasibility study. Radiology. 2001 Apr; 219(1):176–185. [PubMed: 11274554]
80. McDannold N, Vykhodtseva N, Raymond S, Jolesz FA, Hynynen K. MRI-guided targeted blood-brain barrier disruption with focused ultrasound: Histological findings in rabbits. Ultrasound in Medicine & Biology. 2005 Nov; 31(11):1527–1537. [PubMed: 16286030]
81. Treat LH, McDannold N, Vykhodtseva N, Zhang Y, Tam K, Hynynen K. Targeted delivery of doxorubicin to the rat brain at therapeutic levels using MRI-guided focused ultrasound. Int J Cancer. 2007; 121(4):901–907. [PubMed: 17437269]
82. Liu H-L, Hua M-Y, Chen P-Y, Chu P-C, Pan C-H, Yang H-W, et al. Blood-Brain Barrier Disruption with Focused Ultrasound Enhances Delivery of Chemotherapeutic Drugs for Glioblastoma Treatment 1. Radiology. 2010 May; 255(2):415–425. [PubMed: 20413754]
83. Wei, K-C.; Chu, P-C.; Wang, H-YJ.; Huang, C-Y.; Chen, P-Y.; Tsai, H-C., et al. Focused Ultrasound-Induced Blood–Brain Barrier Opening to Enhance Temozolomide Delivery for Glioblastoma Treatment: A Preclinical Study. In: He, X., editor. PLoS ONE. Vol. 8. 2013 Mar 19. p. e58995
84. Schlesinger D, Benedict S, Diederich C, Gedroyc W, Klibanov A, Larner J. MR-guided focused ultrasound surgery, present and future. Med Phys. 2013; 40(8):080901. [PubMed: 23927296]

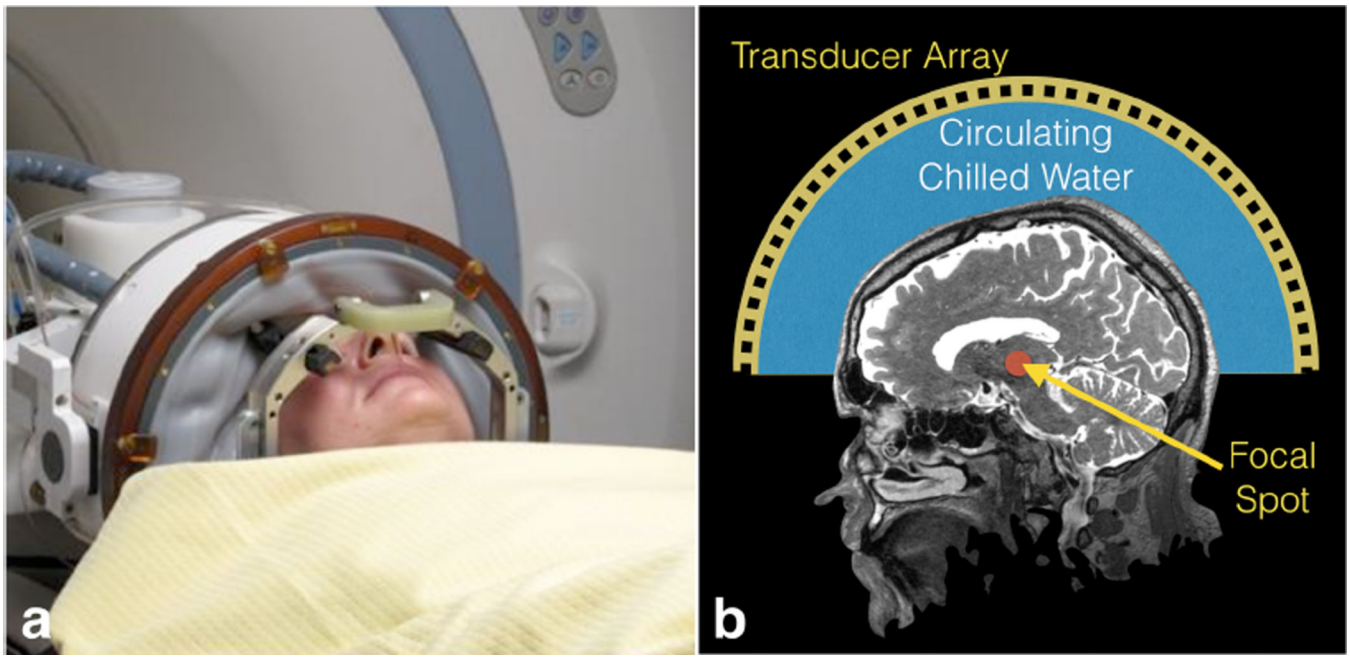

Figure 1.

Photograph and schematic of the InSightec Exablate transcranial focused ultrasound system. A membrane holds in the water between the transducer and the patient head. The patient is fixed to the table by the frame, while the transducer can move independently in order to place the target as close as possible to the geometric center of the hemisphere.

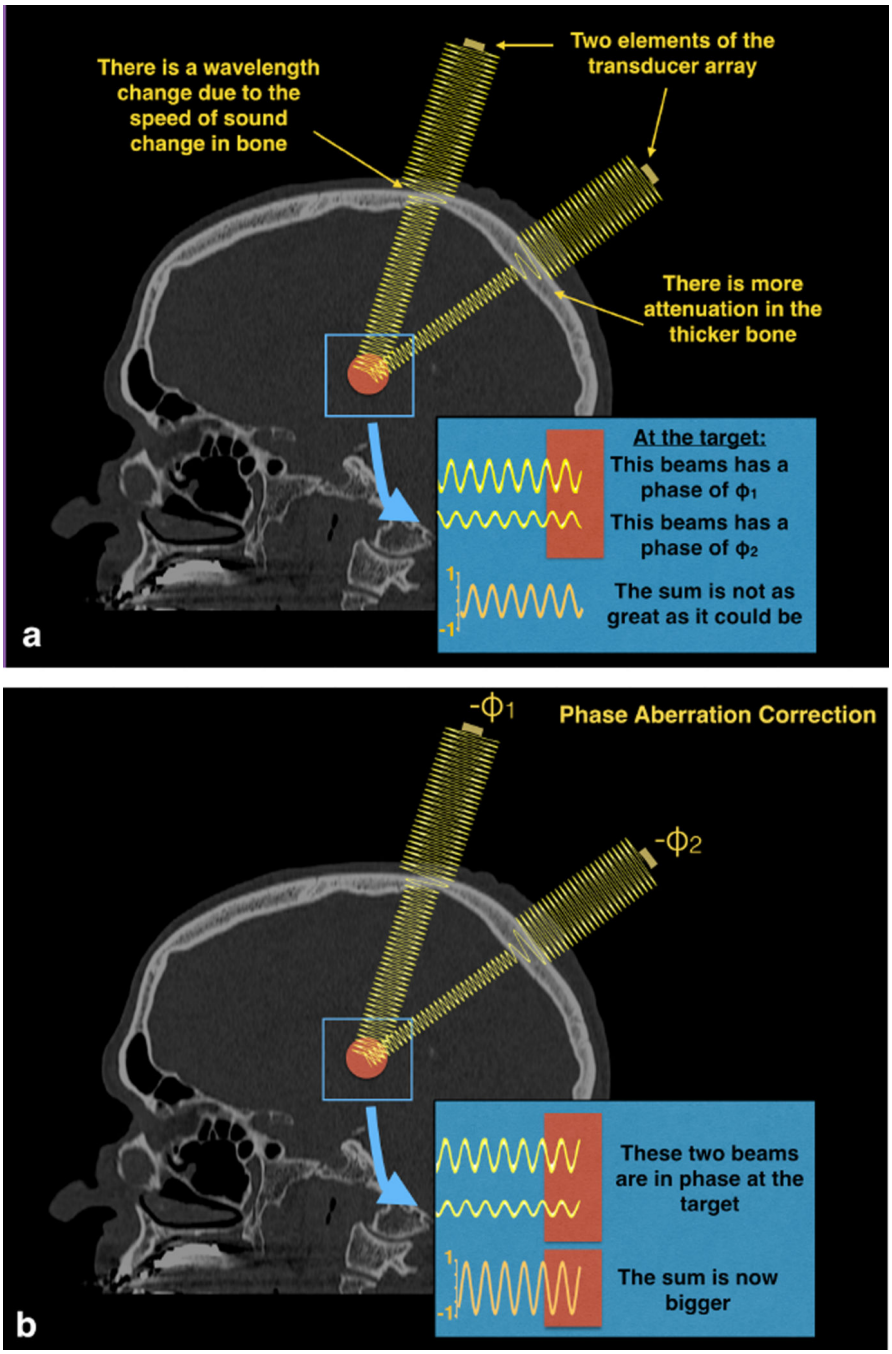

Figure 2.

Two example beams traveling through water, a simplified bone model with a single elevated velocity, then soft tissue to the target. The increased speed of sound through bone results in a change in wavelength. These two beams pass through different lengths of bone, resulting in differences in phase when the beams hit the target. Such differences in phase mean that the beams do not add constructively and the resulting temperature rise is lower than it could be. Phase aberration correction methods estimate this phase and apply the negative of it to each transducer element.

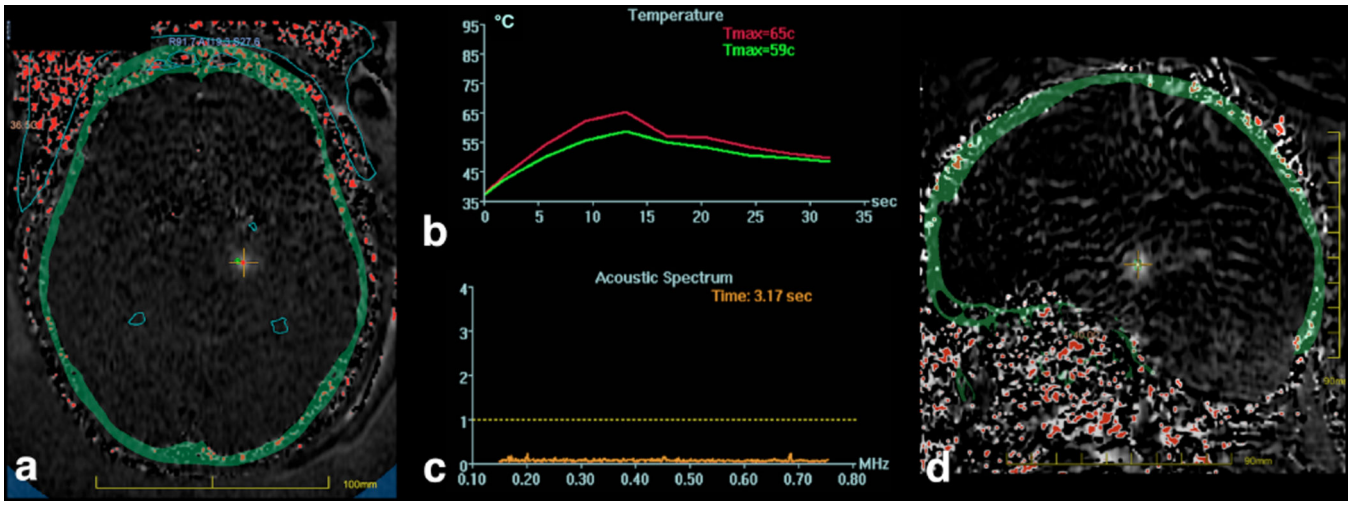

Figure 3.

MR temperature maps in a and d derived from the change in proton resonant frequency seen with temperature. The skull is overlaid on the temperature image in green. A cross hair is placed at the location of the focal spot, with the maximum temperature within a 3×3 region of interest plotted in b), along with the average in the 3×3 pixel region of interest. These curves demonstrate an exponential rise in temperature during the sonication, and the exponential decay in temperature after the sonication is ended.

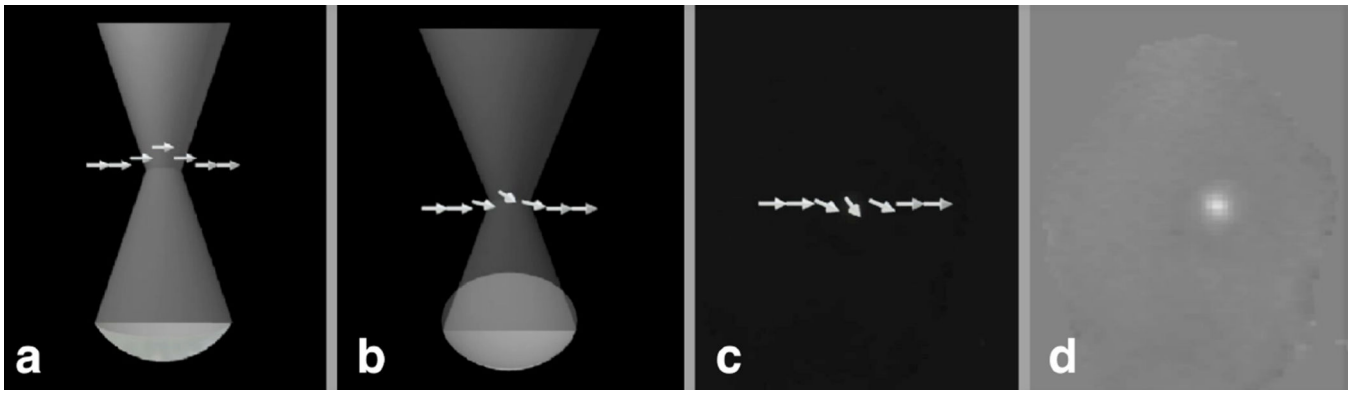

Figure 4.

a) MR-ARFI relies on the acoustic radiation force at the focus displacing the spins. This displacement is encoded into the phase of the spins b) and c) and therefore the phase of the image d). These images were collected in an ex vivo porcine brain as described in Kaye et al.

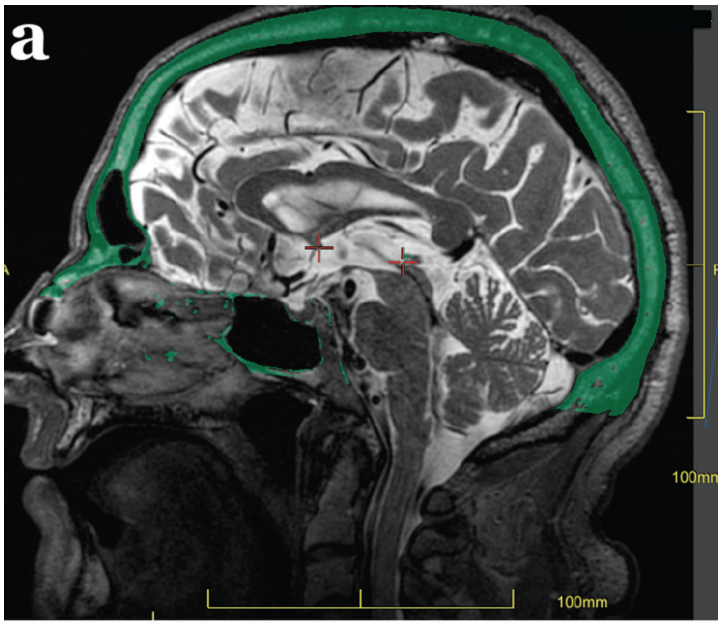

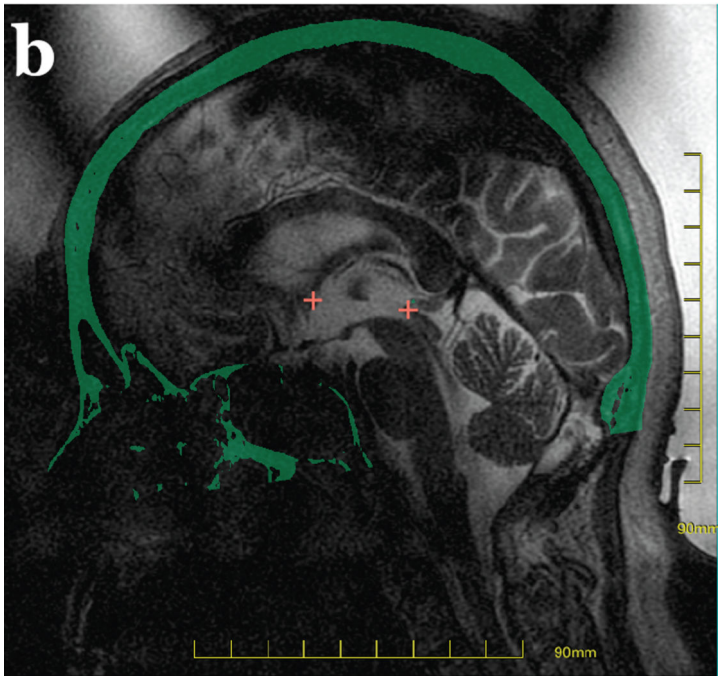

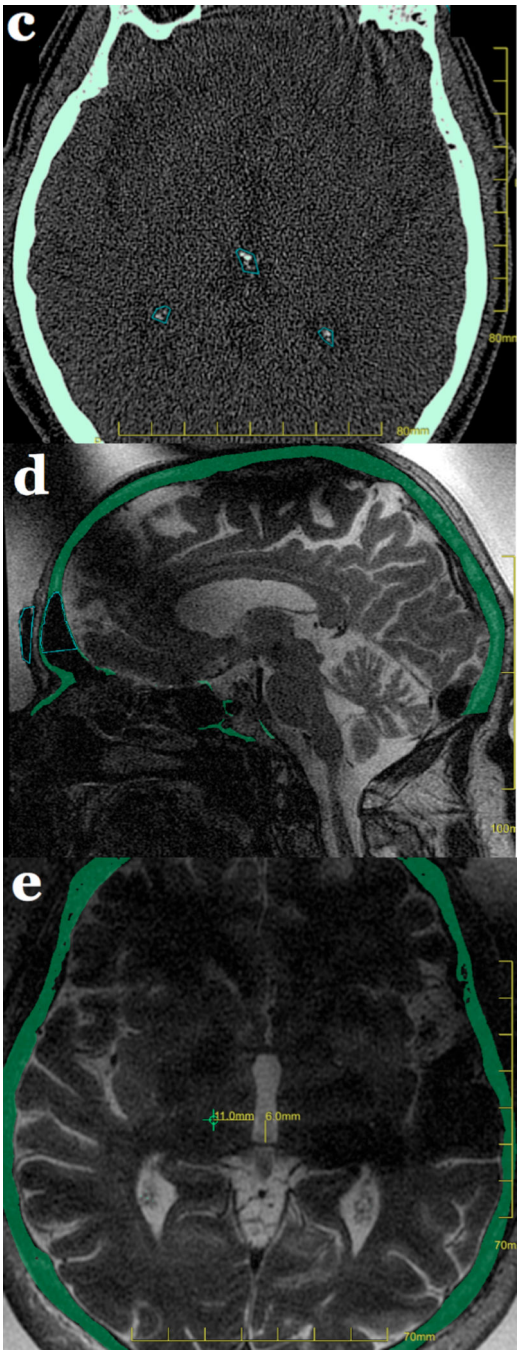

Figure 5.

Treatment planning images. Sagittal MR images acquired before treatment (a) and on the treatment day (b) are co-registered using the CT overlay (in green). The anterior and posterior commissures are marked in red. “No pass” zones in blue mark intrancranial calcifications in the choroid plexus, pineal gland, falx, basal ganglia or vessels on the CT (c), as is air in the sinuses, and air trapped between the membrane and scalp is marked on the treatment day MRI (d). Anatomic measurements for targeting the Vim nucleus of the

thalamus provide a starting point for essential tremor treatments (e), with final targeting confirmed using intra-procedural neurological feedback from the awake patient.

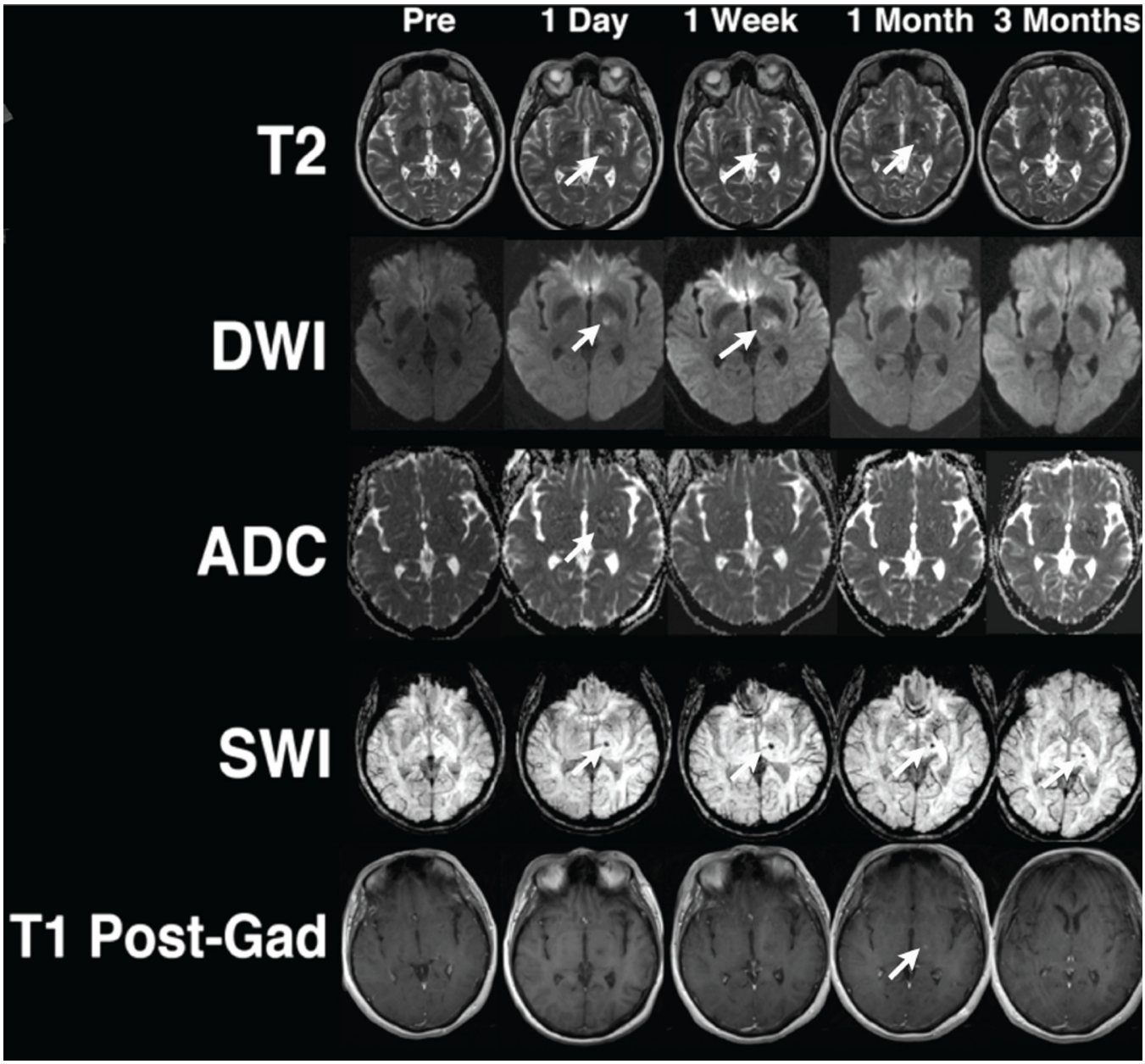

Figure 6.

Conventional MR imaging features after MRgFUS lesioning of the left ventralis intermedius nucleus (Vim) of the thalamus in a right-handed patient with essential tremor. The MRgFUS lesion appears on T2-weighted images at 24 hours and initially restricts diffusion. It demonstrates faint enhancement at 1 month, and the cavity collapses by 3 months. Blood product staining is seen immediately after the MRgFUS treatment and persists over time.

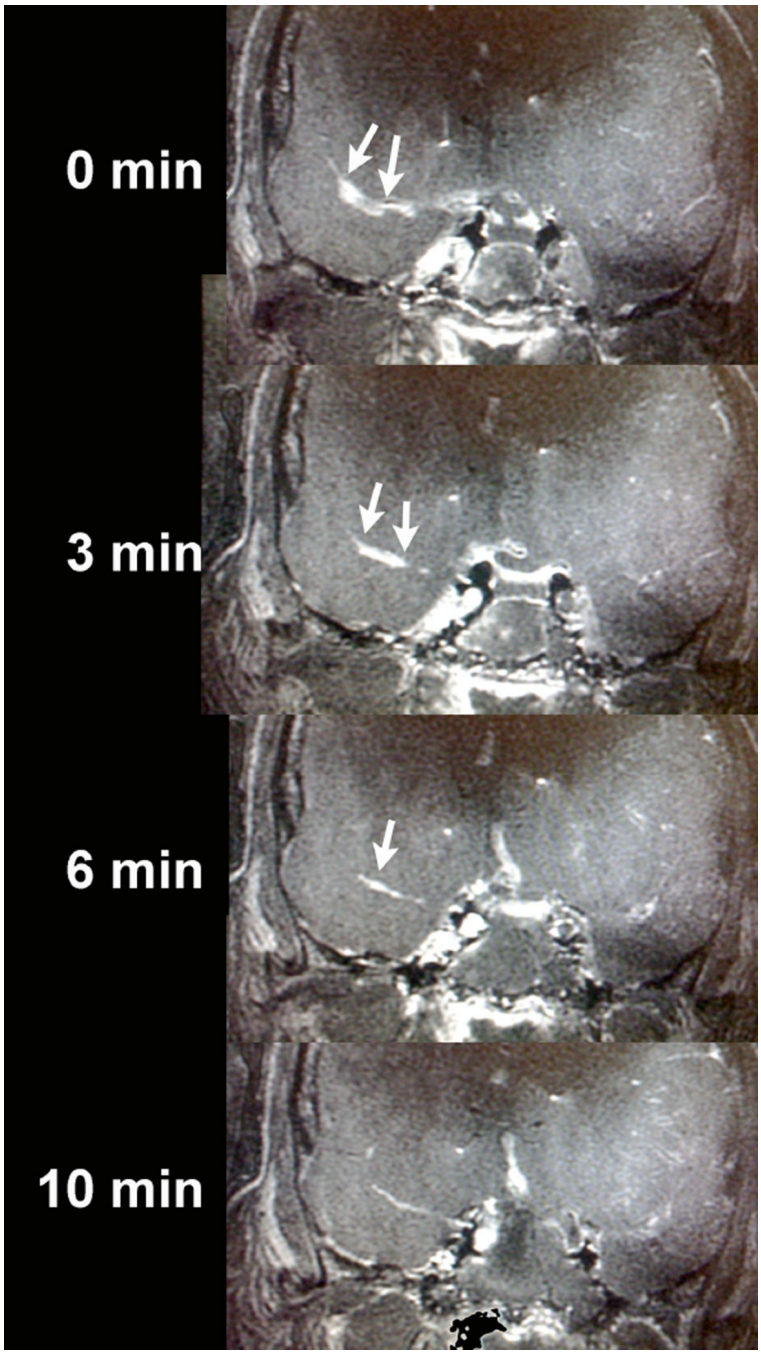

Figure 7.

A clot was induced in the M1 segment of the right middle cerebral artery by injecting thrombin through an endovascular microcatheter introduced through the femoral artery in a fresh human cadaver, and flow in the arteries was maintained by a saline pumping system. MRgFUS targeted the right M1 clot (arrows) and with a total of 4 sonications, the clot was completely sonothrombolyzed over 10 minutes.